CdSe/ZnS QDs Embedded in Cellulose Triacetate Films with Hydrophilic Surfaces

Tiffany Abitbol and Derek Gray*

Department of Chemistry, McGill University, Pulp and Paper Building, 3420 University Street, Montreal, Quebec H3A 2A7, Canada

Received February 13, 2007. Revised Manuscript Received May 17, 2007

Quantum dot (QD)/polymer composite films were prepared by solvent casting suspensions of CdSe/ZnS semiconductor nanoparticles in cellulose triacetate (CTA) solution. The common solubilities of the organic ligands capping the QDs and of the polymer permitted the direct addition of QDs into the CTA casting solution. The films were robust, with typical thicknesses of 0.05 mm, and possessed the optical properties characteristic of QDs. The emission wavelength of the QD/CTA films shifted with time but eventually reverted toward its original value. This effect was attributed to changes in humidity and solvent content of the films. Transmission electron microscopy (TEM) images of QD/CTA films revealed that the QDs were well-dispersed within the CTA film matrix. The selective alkaline hydrolysis of QD/CTA films in 0.1 M NaOH over 24 h resulted in the surface conversion of CTA to regenerated cellulose. X-ray photoelectron spectroscopy (XPS) and attenuated total reflectance Fourier transform infrared spectroscopy (ATR-FTIR) were employed to study the surface composition of the films and transmission mode Fourier transform infrared spectroscopy was used to study the bulk composition. Optical properties of the films were probed both before and after the hydrolysis reaction using fluorescence spectroscopy and were found generally unaltered. The cellulose surfaces of the alkaline-treated films should allow facile incorporation into paper sheets.

Introduction

The incorporation of semiconductor nanoparticles into polymer matrices is an active field of research motivated in general by the development of novel optical devices.[1−5] Here, we describe the preparation of transparent polymer films embedded with semiconductor nanoparticles. The films exhibit the size-quantized optical effects characteristic of semiconductor nanoparticles.

Semiconductor nanoparticle/polymer composites have been achieved by two general methods: (1) the in situ synthesis of nanoparticles in either polymer solution[6−9] or film[10−15] and (2) the ex situ synthesis of nanoparticles and their subsequent incorporation into either monomer or polymer solution[3,16−22] or film.[23−26] Experimental approaches to the ex situ method include the covalent linkage of nanoparticle surface ligands to polymer molecules,[6,27] layer by layer (LBL) assembly of polymer and nanoparticles,[23−26] and the addition of colloidal nanoparticles directly into polymer solution.[19,20,22] Both the in situ and ex situ approaches highlight the importance of the organic ligands tethered to the surface of

* Corresponding author. E-mail: derek.gray@mcgill.ca.

(1) Colvin, V. L.; Schlamp, M. C.; Alivisatos, A. P. *Nature* **1994**, *370*, 354−357.
(2) Beecroft, L. L.; Ober, C. K. *Chem. Mater.* **1997**, *9*, 1302−1317.
(3) Lee, J.; Sundar, V. C.; Heine, J. R.; Bawendi, M. G.; Jensen, K. F. *Adv. Mater.* **2000**, *12*, 1102−1105.
(4) Schlecht, S.; Tan, S.; Yosef, M.; Dersch, R.; Wendorff, J. H.; Jia, Z.; Schaper, A. *Chem. Mater.* **2005**, *17*, 809−814.
(5) Dabbousi, B. O.; Bawendi, M. G. *Appl. Phys. Lett.* **1995**, *66*, 1316−1318.
(6) Hirai, T.; Miyamoto, M.; Komasawa, I. *J. Mater. Chem.* **1999**, *9*, 1217−1219.
(7) Hirai, T.; Watanabe, T.; Komasawa, I. *J. Phys. Chem. B* **1999**, *103*, 10120−10126.
(8) Ruan, D.; Huang, Q.; Zhang, L. *Macromol. Mater. Eng.* **2005**, *290*, 1017−1024.
(9) Khanna, P. K.; Gokhale, R. R.; Subbarao, V. V. V. S.; Singh, N.; Jun, K.-W.; Das, B. K. *Mater. Chem. Phys.* **2005**, *94*, 454−459.
(10) Antolini, F.; Di Luccio, T.; Re, M.; Tapfer, L. *Cryst. Res. Technol.* **2005**, *40*, 948−954.
(11) Yuan, Y.; Cabasso, I.; Fendler, J. H. *Macromolecules* **1990**, *23*, 3198−3200.
(12) Yuan, Y.; Fendler, J. H.; Cabasso, I. *Chem. Mater.* **1992**, *4*, 312−318.
(13) Wang, S.; Yang, S. *Langmuir* **2000**, *16*, 389−397.
(14) Wang, Y.; Mahler, W. *Opt. Commun.* **1987**, *61*, 233−236.
(15) Olshavsky, M. A.; Allcock, H. K. *Chem. Mater.* **1997**, *9*, 1367−1376.
(16) Song, H.; Lee, S. *Nanotechnology* **2007**, *18*, 1−6.
(17) Dabbousi, B. O.; Bawendi, M. G.; Onitsuka, O.; Rubner, M. F. *Appl. Phys. Lett.* **1995**, *66*, 1316−1318.
(18) Sheng, W.; Kim, S.; Lee, J.; Kim, S.-W.; Jensen, K.; Bawendi, M. G. *Langmuir* **2006**, *22*, 3782−3790.
(19) Yanagida, S.; Enokida, T.; Shindo, A.; Shiragami, T.; Ogata, T.; Fukumi, T.; Sakaguchi, T.; Mori, H.; Sakata, T. *Chem. Lett.* **1990**, 1773−1776.
(20) Tamborra, M.; Striccoli, M.; Comparelli, R.; Curri, M. L.; Petrella, A.; Agostiano, A. *Nanotechnology* **2004**, *15*, S240−S244.
(21) Fogg, D. E.; Radzilowski, L. H.; Dabbousi, B. O.; Schrock, R. R.; Thomas, E. L.; Bawendi, M. G. *Macromolecules* **1997**, *30*, 8433−8439.
(22) Rong, M. Z.; Zhang, M. Q.; Liang, H. C.; Zeng, H. M. *Appl. Surf. Sci.* **2004**, *228*, 176−190.
(23) Constantine, C. A.; Gattas-Asfura, K. M.; Mello, S. V.; Crespo, G.; Rastogi, V.; Cheng, T.-C.; DeFrank, J. J.; Leblanc, R. M. *J. Phys. Chem. B* **2003**, *107*, 13762−13764.
(24) Constantine, C. A.; Gattas-Asfura, K. M.; Mello, S. V.; Crespo, G.; Rastogi, V.; Cheng, T.-C.; DeFrank, J. J.; Leblanc, R. M. *Langmuir* **2003**, *19*, 9863−9867.
(25) Zhang, L.; Zhang, F.; wang, Y.; Claus, R. O. *J. Chem. Phys.* **2002**, *116*, 6297−6304.
(26) Zucolotto, V.; Gattas-Asfura, K. M.; Tumolo, T.; Perinotto, A. C.; Antunes, P. A.; Constantino, C. J. L.; Baptista, M. S.; Leblanc, R. M.; Oliveira, O. N. *Appl. Surf. Sci.* **2005**, *246*, 397−402.

10.1021/cm0704332 CCC: $37.00
Published on Web 07/28/2007

the nanoparticles. The ligands provide the interface between the colloidal nanoparticles and surrounding environment. The nature of the interaction between nanoparticles and a given macromolecular matrix will be mediated by the ligands; for example, nanoparticles passivated with hydrophilic ligands will generally be compatible with aqueous systems.

Cellulose is the most abundant and readily available biopolymer.[28] However, because of its highly crystalline and strongly hydrogen-bonded structure, cellulose does not dissolve in most solvents, and it may be preferable to work with cellulose derivatives, such as cellulose esters soluble in common organics, or to work with aqueous suspensions of colloidal cellulose nanocrystals.[29] The use of cellulose or cellulose derivatives as a matrix for semiconductor nanocrystals has been previously investigated; Ruan et al. reported the in situ synthesis of CdS nanoparticles in cellulose solution and the subsequent casting of CdS/regenerated cellulose films[8] and Yuan et al. have incorporated CdS nanoparticles into polymer blend membranes (PBMs) in which one of the polymeric components of the PBM was cellulose acetate.[11,12] In the present study, CTA, a cellulose derivative in which the hydroxyl groups of cellulose are replaced with acetyl groups, is employed as the polymer matrix for the QDs and as an indirect approach to regenerated cellulose. The role of the CTA polymer was primarily to provide a stable and inert environment for the nanoparticles in a robust, transparent, plastic form and to provide the potential for conversion to cellulose, which may prove useful in some paper-making applications.

The solubility of CTA in common organic solvents allows for the incorporation of appropriately passivated nanocrystals directly into the polymer solution. The QD/CTA films are hydrophobic; that is, the films are composed of hydrophobic polymer embedded with QDs that are passivated with hydrophobic ligands. To make the QD/CTA films compatible with aqueous systems, we chemically modified the CTA film surface to regenerate cellulose. In this study, treatment conditions were employed in order to convert only the film surfaces to regenerated cellulose. Surface hydrolysis to regenerated cellulose allowed for modification of film surface properties while retaining a stable, bulk polymeric matrix for the QDs. The fluorescent, hydrolyzed films may potentially be incorporated into paper products by hydrogen bonding to other cellulose surfaces.

Experimental Section

Materials. Cellulose triacetate (43% acetyl content) and Congo red (MW 697 g/mol) were purchased from Sigma-Aldrich. Commercial suspensions of CdSe/ZnS QDs in toluene with nominal particle sizes ranging from 1.9 to 4.0 nm and nominal concentrations of 0.5−1.18 mg/mL were purchased from Evident Technologies. The QDs were capped with either tri-octyl phosphine oxide (TOPO) or with a proprietary straight 16 carbon chain.

Film Preparation. A 40 g/L CTA solution was prepared by dissolving CTA in a 9:1 dichloromethane:methanol mixed-solvent system. Small volumes (0.1−0.2 mL) of either one or several different-sized QDs were added to a 20−25 mL volume of the CTA solution. A homogeneous distribution of QDs in the casting solution was achieved by vigorously stirring the mixture for 1 h using a vortex mixer. To cast the film, we poured the mixture into a glass Petri dish and left the solvent to evaporate for approximately 24 h in a desiccator or covered with foil under ambient conditions. Transfer to the Petri dish was not quantitative because of the viscous nature of the polymer solution. Finally, the films were carefully peeled off the glass surface. The films were robust, transparent, and had thicknesses on the order of 0.05 mm, depending on the amount of casting mixture used and effectively transferred.

Transmission Electron Microscopy (TEM). TEM images were obtained of QD/CTA films dried onto carbon-coated TEM grids using a Philips CM200 TEM, operated at 200 kV, with a point-to-point resolution of 0.24 nm and line resolution of 0.17 nm.

Alkaline Hydrolysis. To convert the film surfaces to cellulose, the QD/CTA films were submerged in a beaker of either 0.1 M NaOH or 2.4 M NH_4OH over a 24 or 48 h period with continuous stirring. The films were then removed from the alkaline bath and rinsed thoroughly and repeatedly under a flow of distilled water to remove any excess base. Drying was performed either under ambient conditions or in a 110 °C oven for 1 h.

Optical Characterization. UV−vis spectra were obtained with a Cary 300 BIO UV−vis spectrometer (Varian) and emission spectra were recorded on a FluoroMax-2 fluorimeter (Jobin Yvon-Spex). All emission curves were obtained at an excitation wavelength of 350 nm and emission and excitation monochromator slit widths of 1 and 3 nm for solutions and films, respectively.

QD Content. To determine the weight percent QDs in the films, we dissolved a weighed piece of the QD/CTA film in a known volume of a 9:1 dichloromethane:methanol mixture. The mass of QDs in the volume of dissolved film was obtained from Beer−Lambert curves of suspensions of QDs in 10 g/L solutions of CTA.

Bulk Compositional Analysis. To study the bulk composition of the films, we recorded transmission mode Fourier transform infrared spectra of both untreated and alkaline treated films with a Spectrum BX FTIR spectrometer (Perkin-Elmer). The FTIR spectrum was an average of 8 scans obtained at a resolution of 4 cm^{-1}.

Surface Compositional Analysis. Congo red film staining, attenuated total reflectance spectroscopy (ATR-FTIR), and X-ray photoelectron spectroscopy (XPS) were performed to compare the surface composition of untreated and hydrolyzed films. (i) Alkaline-treated films were submerged in 4.8×10^{-4} M solutions of Congo red dissolved in equal parts of water and ethanol. After 15 min, the films were removed from the dye solution and rinsed with copious amounts of distilled water to wash away surplus stain. (ii) ATR-FTIR spectra were obtained using the MIRacle ATR accessory (Pike technologies) in conjunction with a Spectrum BX FTIR spectrometer (Perkin-Elmer). All ATR-FTIR spectra were recorded using a diamond crystal plate and each spectrum was an average of 8 scans with 4 cm^{-1} resolution. A correction was applied in order to take into account the higher penetration depth of the IR beam that occurs at lower frequencies. The depth of penetration (d_p) is expressed in terms of the wavelength of light (λ), the angle of incidence of the IR beam (θ) and by the refractive indices of the crystal (n_1) and sample (n_2)[30]

$$d_p = \lambda/2\pi(n_1^2 \sin^2 \theta_1 - n_2^2)^{1/2}$$

As an example, the depth of penetration of the IR beam into a CTA film at 1730 cm^{-1}, given a 45° angle of incidence and

(27) Nie, Q.; Tan, W. B.; Zhang, Y. *Nanotechnology* **2006**, *17*, 140−144.
(28) Klemm, D.; Philipp, B.; Heinze, T.; Heinze, U.; Wagenknecht, W. *Comprehensive Cellulose Chemistry*, 1st. ed.; Wiley-VCH Verlag GmbH: Weinheim, Germany, 1998; Vol. 1.
(29) Cranston, E. D.; Gray, D. G. *Biomacromolecules* **2006**.
(30) Harrick, N. J. *Internal Reflection Spectroscopy*; Interscience Publishers: New York, 1967.

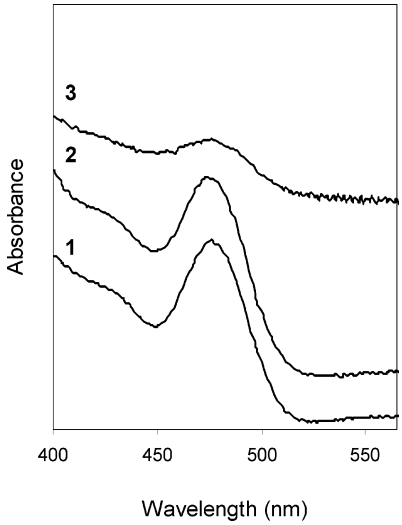

Figure 1. UV−vis spectra of 1.9 nm QDs in three environments: (1) in toluene, (2) in a 10 g/L CTA solution, and (3) embedded in a CTA film. The concentration of QDs in the solution spectra is 0.0057 mg/mL, and the weight percentage of QDs in the film is 0.010 ± 0.002%.

approximate refractive indices of 1.5 for CTA[31] and 2.4 for diamond,[32] is 1.2 μm.

(iii) XPS spectra were recorded of the front and back of five film samples using an AXIS Ultra electron spectrometer (Kratos Analytical), under UHV conditions and equipped with an Al Kα source (12.5 kV, 8 mA). Low-resolution 0.33 eV or 1 eV step survey scans provided qualitative information regarding the overall elemental composition of the film surfaces. The high-resolution 0.1 eV scans were used to resolve the O_{1s} and C_{1s} peaks and quantify the C_{1s} peak components. Atomic concentration percentages for the oxygen and carbon components were obtained by applying the appropriate sensitivity factors ($S = 0.278$ for C_{1s} and $S = 0.780$ for O_{1s}) to the raw peak areas (I) according to the following equation

$$\text{atomic concentration percent}_A = I_A/S_A(I_B/S_B + I_A/S_A)^{-1}$$

In addition to the film samples, XPS spectra were obtained for a piece of Whatman no. 541 filter paper that had been extracted in acetone using a Soxhlet apparatus. The filter paper was intended as a pure cellulose reference.

Results and Discussion

The UV−vis spectrum of a CTA film embedded with 1.9 nm QDs is presented in Figure 1. The spectra of the 1.9 nm QDs in toluene and in a 10 g/L solution of CTA are included for comparison. Although the characteristic first excitonic peak located at ∼474 nm is present in all three curves, the absorbance spectrum of the film is comparatively broadened and structureless and the higher-energy optical transition at ∼430 nm is not at all apparent. Broadening and red-shifting of the QD absorbance spectrum can be understood in terms of the transition from isolated QDs, with localized electronic states, to the delocalized electron−hole states characteristic of nanocrystal clusters, i.e., of close-packed ensembles of several nanocrystals.[33−35] The experimental observation of spectral broadening in the film samples may therefore imply some degree of aggregation of the QDs embedded within CTA. However, this mechanism requires the overlap of QD electronic states and is unlikely to be a dominant process in the current system where the presence of polymer and QD surface ligands will hinder contact between the QDs. In fact, polymer is typically added to QD samples in order to observe the localized states associated with isolated nanoparticles. The noise associated with the solid spectrum makes it difficult to discern the precise peak position and whether the optical transitions are in fact red-shifted in the film and may also contribute to the peak broadening.

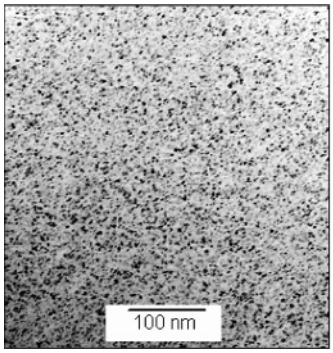

Figure 2. TEM image of CTA film embedded with 1.9 nm QDs. The concentration of CTA solution is 1 g/L and the concentration of QDs in polymer solution is 0.0006 mg/mL.

In general, TEM images showed a relatively homogeneous distribution of the QDs/QD clusters within the CTA films. Consistent with the presence of polymer, no evidence of a regular QD packing arrangement or long-range order is observed. A TEM image of a 1.9 nm QD/CTA film is presented in Figure 2. The film is densely crowded with QDs and there appear to be regions of the film in which several QDs are clustered together; however, the QDs/QD clusters seem to be well-dispersed within the polymer.

The fluorescence spectra of 1.9 nm QDs in a 10 g/L CTA solution and a CTA film are presented in Figure 3. As might be expected from the solution absorbance curves presented in Figure 1, the emission of QDs in 10 g/L CTA solution and in toluene were found to overlap. The emission spectrum of the QD/CTA film has a broad, high-energy tail, centered at ∼430 nm, which is attributed to the crystallinity of CTA polymer.[11,12] In general, the CTA emission is found to be negligible in comparison to the highly luminescent QDs, but obviously, at sufficiently low QD concentrations, this statement will not hold true. QD optical transitions are excited at energies greater than or equal to the band gap; it is therefore possible to excite QDs of different sizes at a single wavelength. The inset of Figure 3 presents the emission of a CTA film embedded with three different sized QDs and establishes the QD/CTA system as appropriate for multiplexing purposes. Further, in a film containing one or more average QD sizes, changing the excitation wavelength will alter the emission intensities, i.e., at a given excitation

(31) In *Polymer Handbook*, 4th ed.; Brandrup, J.; Immergut, E. H.; Grulke, E. A.; Abe, A.; Bloch, D. R., Eds.; John Wiley & Sons: New York, 2005.
(32) *Knovel Critical Tables*; Knovel: Norwich, NY, 2003.
(33) Artemyev, M. V.; Bibik, A. I.; Gurinovich, L. I.; Gapochenko, S. V.; Woggon, U. *Phys. Rev. B* **1999**, *60*, 1504−1506.
(34) Artemyev, M. V.; Woggon, U.; Jaschinski, H.; Gurinovich, L. I.; Gapochenko, S. V. *J. Phys. Chem. B.* **2000**, *104*, 11617−11621.
(35) Micic, O. I.; Ahrenkiel, S. P.; Nozik, A. J. *Appl. Phys. Lett.* **2001**, *78*, 4022−4024.

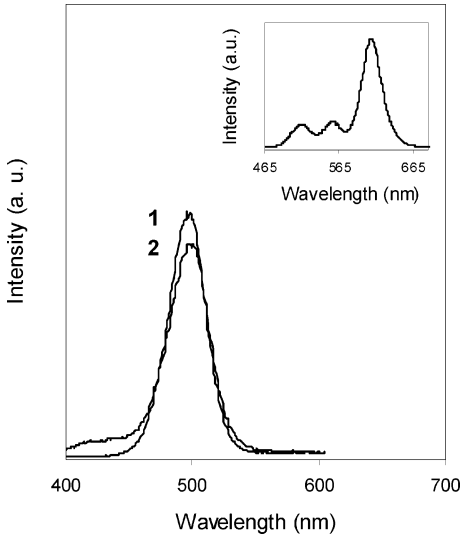

Figure 3. Emission spectra of 1.9 nm QDs in (1) 10 g/L CTA solution and (2) CTA film. The concentration of QDs in the solution spectrum is 0.0133 mg/mL, and the weight percentage of QDs in the film is 0.005 ± 0.003%. The inset is an emission spectrum of a CTA film embedded with 3 different-sized QDs: 2.1, 2.6, and 4.0 nm with weight percents of 0.0171 ± 0.0004%, 0.017 ± 0.003%, and 0.01 ± 0.01%, respectively.

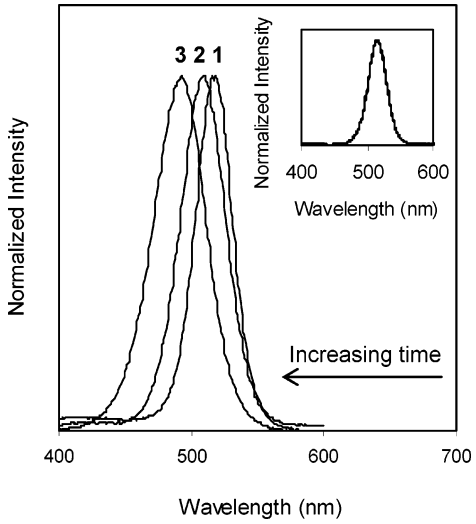

Figure 4. Effect of time on the emission of a 2.1 nm QD/CTA film with 0.006 ± 0.003% QD by weight. Curve (1) was obtained at time *t*, (2) at *t* + 60 days, and (3) at *t* + 187 days. The inset depicts the overlapping emission spectra of the 2.1 nm QDs dispersed in toluene and in 10 g/L CTA to a concentration of 0.021 g/L.

wavelength, different sizes and size distributions of the QDs are excited to varying extents. In the present study, different-sized QDs were incorporated into a single film without any size segregation. In this type of highly fluorescent and densely populated film, some light emitted from the smaller QDs will be absorbed by the larger QDs[3] and Förster resonance energy transfer (FRET) is expected to occur between proximal QDs.[36−39] In general, the overlap between absorbance and emission dictates the likelihood of both radiative and nonradiative energy transfer between QDs. Radiative and nonradiative energy transfer red-shift the emission wavelengths and result in an overrepresentation of the larger-sized, redder QDs and an underrepresentation of the smaller-sized, bluer QDs in the emission profile. Thus, reabsorption of light emitted from the smaller, higher band gap QDs by the larger QDs is possible and will affect the film color that is observed under UV irradiation. In contrast, a more structured film, where the different sized QDs are segregated into separate layers, FRET between different sized QDs would be minimized, allowing greater control of the observed color.[3] It is, however, important to note that in a layered film, radiative energy transfer through the layers and even within a layer containing a single size distribution of QDs is still possible, as is FRET within a given layer.[3]

The stability of the QD/CTA films, stored under ambient conditions in covered plastic Petri dishes, was assessed from fluorescence spectra. In Figure 4, the emission spectra for a CTA film embedded with 2.1 nm QDs, taken at three different times, is presented. Curve 1 was obtained a short time after the film was cast and curves 2 and 3 were recorded 60 days and 187 days later, respectively. The emission of the 2.1 nm QDs in toluene and in a 10 g/L solution of CTA is included for comparison. The characteristic, narrow QD emission peak is retained over time, a good indication that the CTA polymer matrix provides a stable and appropriate environment for the QDs. A relatively large overall blue-shift in the emission wavelength is observed in the films over time and in comparison to the QD emission in solution. Curves 1−3 have emission wavelengths of ∼518, ∼509, and ∼495 nm, respectively, compared to ∼515 nm for the QDs in CTA solution and in toluene. As previously discussed, the initial red-shift of ∼5 nm is most likely due to radiative and nonradiative energy transfer between the QDs, which may be further intensified by aggregation of the semiconductor nanocrystals. We propose that the blue-shift in emission position of the film over time can be attributed to evaporation of residual solvent in the film samples. Trapping QDs in nonfluid, rigid media likely inhibits the relaxational processes of the excited state, resulting in emission from a higher-energy excited state.[40] Over time, as the solvent gradually evaporates from within the films, the environment becomes more condensed and the molecules (residual solvent, polymer, and ligand) surrounding the QDs are less able to undergo the conformational changes necessary to lower the energy of the excited state. It is expected that the emission wavelength will more or less stabilize once solvent evaporation reaches equilibrium; however, for films stored under ambient conditions, humidity will likely continuously affect film environment and consequently emission position. In fact, a fluorescence spectrum of this sample obtained at t1 + 260 days had an emission wavelength of ∼ 513 nm, reflecting further minor fluctuations in the film environment.

A saponification reaction was utilized to modify the film surfaces; the alkaline hydrolysis of CTA to cellulose is depicted in Figure 5. Four alkaline hydrolysis conditions were studied: 24 h in 0.1 M NaOH, 48 h in 0.1 M NaOH, 24 h in 2.4 M NH_4OH, and 48 h in 2.4 M NH_4OH. Congo red

(36) Clapp, A. R.; Medintz, I. L.; Mattoussi, H. *ChemPhysChem* **2006**, *7*, 47−57.
(37) Crooker, S. A.; Hollingsworth, J. A.; Tretiak, S.; Klimov, V. I. *Phys. Rev. Lett.* **2002**, *89*, 186802−186801−186802−186804.
(38) Kagan, C. R.; Murray, C. B.; Nirmal, M.; Bawendi, M. G. *Phys. Rev. Lett.* **1996**, *76*, 1517−1520.
(39) Kagan, C. R.; Murray, C. B.; Bawendi, M. G. *Phys. Rev. B* **1996**, *54*, 8633−8643.
(40) Sharma, A.; Schulman, S. G. *Introduction to Fluorescence Spectroscopy*, 1st ed.; John Wiley and Sons: New York, 1999.

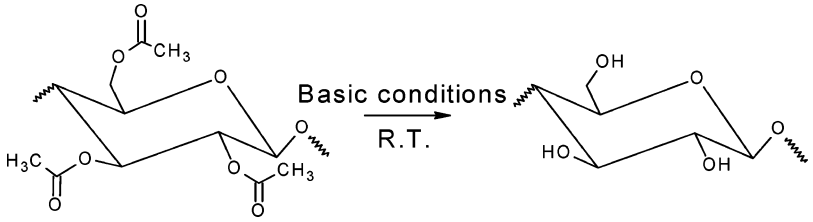

Figure 5. Alkaline hydrolysis of cellulose triacetate to cellulose. Four ambient (RT) conditions were studied: (1) 24 h in 2.4 M NH_4OH, (2) 48 h in 2.4 M NH_4OH, (3) 24 h in 0.1 M NaOH, and (4) 48 h in 0.1 M NaOH.

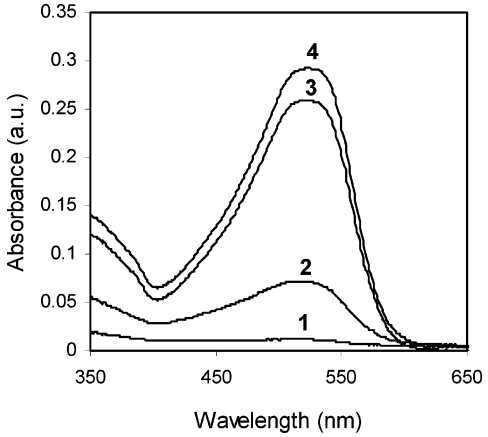

Figure 6. UV−vis absorbance spectra of CTA films that have been alkaline-treated and stained in Congo red dye. Hydrolysis conditions: (1) 24 h in 2.4 M NH_4OH, (2) 48 h in 2.4 M NH_4OH, (3) 24 h in 0.1 M NaOH, and (4) 48 h in 0.1 M NaOH.

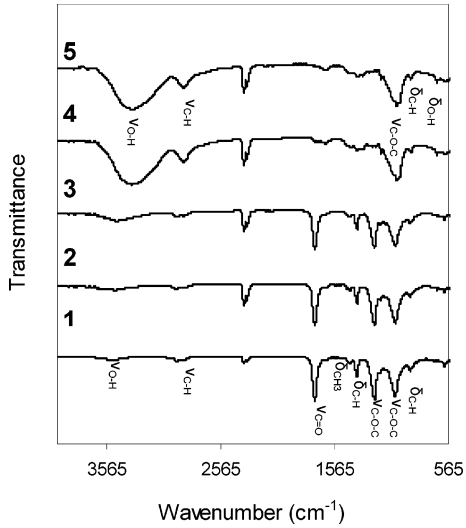

Figure 7. ATR-FTIR spectra of alkaline treated CTA film embedded with 1.9 nm QDs (weight percent, 0.010 ± 0.002%). Hydrolysis conditions: (1) untreated film, (2) 24 h in 2.4 M NH_4OH, (3) 48 h in 2.4 M NH_4OH, (4) 24 h in 0.1 M NaOH, and (4) 48 h in 0.1 M NaOH. The spectra of the samples treated in NaOH are characteristic of cellulose.

dye has a high affinity for cellulose and can be used as a qualitative measure for the degree of acetyl desubstitution.[41,42] The azo moieties of Congo red hydrogen bond with the hydroxyl groups of cellulose, staining cellulose film surfaces red; no analogous interaction exists between Congo red and CTA. The Congo red absorbance peak at ∼515 nm was used as a marker for the hydrolysis reaction; the more stained a film surface appears, the larger the extent of CTA hydrolysis. From the curves presented in Figure 6, it is apparent that all treatment conditions result in some degree of CTA deacetylation, with the CTA films treated in 0.1 M NaOH experiencing the most significant conversion to cellulose.

However, little information is provided from the Congo red results regarding the depth of hydrolysis. To better assess the depth to which the samples were deacetylated, we performed ATR-FTIR analysis on CTA films incorporating 1.9 nm QDs, which had undergone the previously listed hydrolysis treatments. IR spectra of films embedded with QDs appear identical to spectra of CTA films that do not incorporate the QDs. Infrared absorbance can be used to differentiate between cellulose acetates and regenerated cellulose;[41−44] most markedly, the carbonyl stretch at ∼1730 cm^{-1} is absent in the cellulose spectrum, whereas the hydroxyl group absorbance at ∼3300−3450 cm^{-1} is increased. A diamond crystal plate was used in the ATR-FTIR experiments. The depth of penetration (d_p) of the IR beam into the sample is wavelength dependent and varies from 0.5 to 4 μm for the given system, in the spectral range of 4000−565 cm^{-1}. The spectrum is therefore representative of the average composition of the sample at surface depths ranging from 0.5 to 4 μm. From the spectra presented in Figure 7 and in particular as indicated by carbonyl stretch at 1730 cm^{-1}, the 0.1M NaOH treated samples are on average composed of cellulose to a depth of at least 1.2 μm into the film surfaces. The condition of 2.4 M NH_4OH proves insufficient for deacetylation even at the relatively shallow depth of 1.2 μm. We reported the successful deacetylation of CTA films in 2.6 M NH_4OH,[42] but the previous work described shear-cast CTA films that were much thinner than the solvent-cast films of the current study. The Congo red and ATR-FTIR results are complimentary; treatment in 0.1 M NaOH for 24 h is sufficient for surface deacetylation and little is gained by an additional 24 h of treatment; in comparison to the NaOH conditions, reaction in NH_4OH is not extensive. Tables 1 and 2 include a detailed assignment of the infrared absorption peaks for the CTA and regenerated cellulose films.[8,43−47]

Table 1. Important Infrared Absorption Bands for CTA Films

wavenumber (cm^{-1})	band assignment	refs
890	δ_{C-H}	44
1024	ν_{C-O-C} (pyranose)	43, 44, 47
1210	ν_{C-O-C} (ester)	43, 44, 46
1365	δ_{C-H}	44, 47
1420	δ_{CH3} (α)	44, 47
1730	$\nu_{C=O}$	43, 44, 47
2872, 2932	ν_{C-H}	43, 44, 46, 49
3460	ν_{O-H}	44, 47

(41) Braun, J. L.; Kadla, J. F. *Biomacromolecules* **2005**, *6*, 152−160.
(42) Ritcey, A. M.; Gray, D. G. *Biopolymers* **1988**, *27*, 1363−1374.
(43) Chen, Y.; Xiong, X.-P.; Yang, G.; Zhang, L.-N.; Lei, S.-L.; Liang, H. *Chin. J. Polym. Sci.* **2002**, *20*, 369−375.
(44) Ilharco, L. M.; Brito de Barros, R. *Langmuir* **2000**, *16*, 9331−9337.

Table 2. Important Infrared Absorption Bands for Regenerated Cellulose Films

wavenumber (cm^{-1})	band assignment	refs
600	δ_{O-H}	45
890	δ_{C-H}	8, 44, 45
988	ν_{C-O-C} (pyranose)	8, 43, 45, 46
2850	ν_{C-H}	45, 46
3300	ν_{O-H}	8, 45, 46

The FTIR transmission spectra presented in Figure 8 show that the bulk of the deacetylated samples remain cellulose triacetate, as indicated by the persistence of the carbonyl absorbance peak at all reaction conditions. Thus, the hydrolysis reaction, as inferred from the ATR-FTIR results above, must occur only in the surface region and does not significantly penetrate into the film. The spectral interpretation presented in Table 1 and 2 still applies, although the peaks located at frequencies lower than ~1500 cm^{-1} are not very well resolved.

It was important to determine whether the alkaline treatment of the QD/polymer films resulted in optical degradation of the QDs. In Figure 9, the emission of a film that has been hydrolyzed in 0.1 M NaOH for 24 h is compared to the emission of the same film prior to alkaline treatment. The apparent increase in intensity after NaOH treatment is not significant; the variation in the emission curves is attributed to the uneven thicknesses of the solvent-cast films. For example, when the thickness of a single film embedded with 1.9 nm QDs was measured 46 times at random film locations, it was found to vary from 0.13 mm to 0.036 mm, with an average thickness of 0.071 ± 0.007 mm. In general, an increase in the emission intensity with film thickness was observed. Film thickness decreased slightly upon 0.1 M NaOH hydrolysis, but it was difficult to quantify the change, if any, in emission intensity because of the large variation associated with the average emission intensity of a small film area (approximately 1 cm^2) of a given average thickness. Interestingly, the emission wavelength post-alkaline treatment was blue-shifted in comparison to the wavelength prior to hydrolysis; the aforementioned film incorporating 1.9 nm QDs experienced a pronounced decrease in average film thickness to 0.019 ± 0.003 mm and a shift in emission wavelength from ~501 to ~483 nm. As previously discussed, the blue-shift may be due to emission from a higher-energy excited state as a consequence of the reduction in film thickness upon hydrolysis.

Quenching of QD emission was observed for films treated in 2.4 M NH_4OH. To further assess the effect of alkaline on QD emission, we added small amounts of the 1.9 nm QD suspensions to 0.1 M NaOH and 2.4 M NH_4OH solutions, and a film embedded with 2.1 nm QDs was suspended above a concentrated bath of NH_4OH. As indicated by observation under UV light, the emissions from all three samples were entirely quenched within a 24 h period. It is therefore reasonable to conclude that exposure to alkali quenches QD emission and that the CTA polymer matrix adequately shields

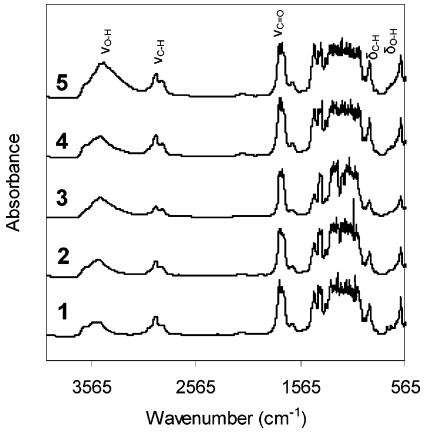

Figure 8. FTIR spectra of alkaline-treated CTA film embedded with 1.9 nm QDs (weight percent of 0.010 ± 0.002%). Hydrolysis conditions: (1) untreated film, (2) 24 h in 2.4 M NH_4OH, (3) 48 h in 2.4 M NH_4OH, (4) 24 h in 0.1 M NaOH, and (5) 48 h in 0.1 M NaOH. Regardless of treatment conditions, all samples exhibit a spectrum characteristic of cellulose triacetate.

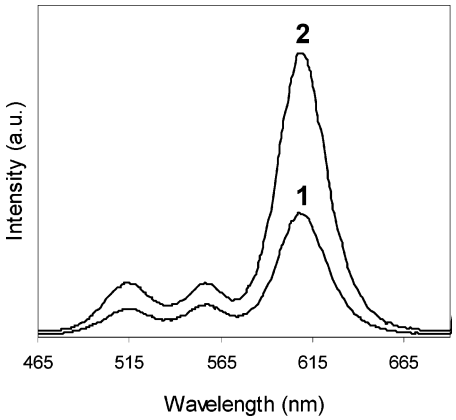

Figure 9. Emission of film embedded with QDs (1) before alkaline treatment, and (2) post-treatment in 0.1 M NaOH. The film is embedded with 3 different sized QDs: 2.1, 2.6, and 4.0 nm with weight percents of 0.017 ± 0.004%, 0.017 ± 0.003%, and 0.01 ± 0.01%, respectively.

the embedded QDs from quenching by the NaOH solution. However, the emission of films exposed to aqueous NH_4OH and ammonia was quenched, indicating that the accessibility and depth of action of NH_4OH/ammonia into the films is significant compared to NaOH treatment. Hence, all subsequent deacetylation reactions were performed with 0.1 M NaOH over 24 h.

XPS was used to estimate the surface conversion of CTA to cellulose. The fronts and backs of six different samples were analyzed; a CTA film, a CTA film embedded with 1.9 nm QDs (QD content estimated at 0.02 wt %) referred to as film C, a deacetylated CTA film, a sheet of Whatman no. 1 filter paper, and two deacetylated films embedded with 2.1 nm QDs, designated deacetylated films A and B. Deacetylated films A and B were cast from the same suspension of QDs in polymer and therefore had an identical weight percent QDs in CTA, 0.023 ± 0.009%. From the survey scan results of all six samples, the only elements present in significant concentrations were carbon and oxygen. Trace amounts of silicon were detected in most samples, excluding the front surface of the hydrolyzed CTA film, the filter paper, and the back surface of the CTA film. Interestingly, XPS did not detect the inorganic elements Cd, Se, Zn, and S, which

(45) Ilharco, L. M.; Garcia, A. R.; Lopes da Silva, J.; Vieira Ferreira, L. F. *Langmuir* **1997**, *13*, 4126−4132.
(46) Kemp, W. *Organic Spectroscopy*, third ed.; Macmillian: London, 1975.
(47) Kondo, T.; Sawatari, C. *Polymer* **1996**, *37*, 393−399.

Table 3. Atomic Concentration Percentages Obtained from XPS of Five Cellulosic Samples[a]

	atomic concentration percents				
sample	C	O	C1	O/C	C1 /(C2+C3+C4)
filter paper	57.4 ± 0.4	42.6 ± 0.4	3.0 ± 0.5	0.74 ± 0.01	0.0031 ± 0.006
hydrolyzed CTA	61 ± 1	39 ± 1	12 ± 3	0.65 ± 0.02	0.14 ± 0.04
hydrolyzed A	63.4 ± 0.7	36.6 ± 0.7	31 ± 2	0.58 ± 0.01	0.45 ± 0.03
hydrolyzed B	64 ± 1	36 ± 1	25 ± 1	0.57 ± 0.02	0.34 ± 0.02
CTA	63.8 ± 0.4	36.2 ± 0.4	26 ± 4	0.57 ± 0.01	0.35 ± 0.05
untreated C	63.7 ± 0.9	36.3 ± 0.9	28 ± 3	0.57 ± 0.02	0.39 ± 0.04
theoretical cellulose	54.55	45.45	0	0.83	0
theoretical CTA	59.62	40.38	24.60	0.68	0.33

[a] The theoretical values for CTA were calculated for commercial CTA with an acetyl content of 43.38%. Samples A and B are alkaline-treated CTA films embedded with 2.1 nm QDs at a weight percent of 0.023 ± 0.009%. The hydrolyzed films were all treated in 0.1 M NaOH over 24 h. Film C is an untreated CTA film that has 1.9 nm QDs dispersed within a weight percent of 0.02%.

comprise the QDs; this may be evidence for the successful incorporation of QDs well within the film bulk or may indicate that the low concentration of QDs within the photoelectron escape depth is beyond detection. The survey results may, however, include a contribution from the hydrocarbon QD ligands to the C(1s) signal.

To attempt a quantitative differentiation of samples, we considered the contributions of the molecular species to the total oxygen O(1s) and carbon C(1s) XPS signals and the component C1, C2, C3, and C4 carbons. The labels C1, C2, C3, and C4 refer to a carbon with no oxygen bonds, a carbon with a single oxygen bond, a carbon with two oxygen bonds, and a carbon with three oxygen bonds, respectively.[48] The atom concentrations and binding energies of the C1, C2, C3, and C4 peaks are obtained by resolving the overall carbon 1s peak into its component carbons. In the high-resolution scans of the cellulose samples, a small tail (in all cases, ≤1.95 atomic concentration percent) is observed at a slightly upfield bonding energy from the main C3 peak. The small tail is considered to be part of the C3 peak and not a minor C4 peak.[49] Similarly, for the CTA samples, two nearly overlapping peaks are combined to obtain the C1 atomic concentration percentage.

The ratios O/C and C1/(*C*2+C3+C4) are characteristic of either cellulose or CTA. Cellulose has 5 oxygens and 6 carbons per repeat unit (O/C = 0.83), and with three acetyl groups per unit, CTA has 8 oxygens and 12 carbons per repeat unit (O/C = 0.67). In addition, the C1/(C2+C3+C4) ratio is 0 for cellulose with no C1 carbons, but 0.33 for CTA with a degree of acetyl substitution of 3. In our commercial CTA sample with a percent acetyl content of 43.38%, the actual number of acetyl groups and hydroxyl groups per repeat unit is 2.91 and 0.10, respectively. The corresponding numbers of total carbons, total oxygens, and C1 carbons per repeat unit are 11.81, 8.0, and 2.91, respectively, giving a theoretical O/C ratio of 0.68 and a C1/(C2+C3+C4) ratio of 0.326.

Surface contamination by hydrocarbon impurities often causes the measured O/C values to be lower (and C1 values to be higher) than expected.[50] The XPS results are presented in Table 3. Results for the filter paper and CTA are in reasonable agreement with literature values,[48,51] but deviate from the theoretical values in the manner expected for the presence of carbon-rich material at the surface.

The XPS evidence for surface carbon-rich contaminants is more marked for the hydrolyzed CTA films and particularly for the samples containing quantum dots. The ATR-FTIR evidence discussed above suggests that the surface of the hydrolyzed films is essentially pure cellulose, but the observed O/C ratios (0.57−0.65) for the much thinner surface layer sampled by XPS indicates the presence of carbon-rich material. The nature of the material is not known in the case of the hydrolyzed cellulose acetate, but we speculate that some of the TOPO or hydrocarbon surfactants used to stabilize the QD suspensions may leach to the cellulose surface. However, regardless of QD content, the hydrolyzed films experience the most significant surface contamination because of the increased manipulation of these films during alkaline treatment.

Conclusion

Stabilized CdSe/ZnS semiconductor nanoparticles may be incorporated in cellulose triacetate films with essentially unaltered fluorescence characteristics. The solvent-cast films protect and facilitate handling of the quantum dots, and surface hydrolysis of the CTA should facilitate utilization of the films in aqueous media.

Acknowledgment. We thank NSERC Canada and Paprican for financial support, the Centre for Self-Assembled Chemical Structures (CSACS) for laboratory access, A. Lejeune (UQTR) for XPS data acquisition and Xue Dong Ling (McGill) for TEM imaging. Helpful direction from P. Kambhampati and practical insight from Nilgun Ulkem are acknowledged.

CM0704332

(48) Dorris, G. M. G. D. G. *Cellul. Chem. Technol.* **1978**, *12*, 9−23.
(49) Edgar, C. D.; Gray, D. G. *Cellulose* **2003**, *10*, 299−306.
(50) Johansson, L.-S.; Campbell, J. M.; Koljonen, K.; Stenius, P. *Appl. Surf. Sci.* **1999**, *144−145*, 92−95.
(51) Riekerink, M. B. O.; Engbers, G. H. M.; Wessling, M.; Feijen, J. *J. Colloid Interface Sci.* **2002**, *245*, 338−348.